Available online at www.sciencedirect.com
ScienceDirect
Scripta Materialia 57 (2007) 771–774
Scripta MATERIALIA
www.elsevier.com/locate/scriptamat

Enhanced anatase-to-rutile phase transformation without exaggerated particle growth in nanostructured titania–tin oxide composites

Krishnankutty-Nair P. Kumar,[a,b,d,*] Derek J. Fray,[a] Jalajakumari Nair,[c] Fujio Mizukami[c] and Tatsuya Okubo[d]

[a] *Department of Materials Science and Metallurgy, University of Cambridge, Pembroke Street, Cambridge CB2 3QZ, UK*
[b] *University of Texas at Dallas, Richardson, TX 75083, USA*
[c] *Research Center for Compact Chemical Process, AIST, 4-2-1, Nigatake, Miyagino-ku, Sendai, Miyagi 983-8551, Japan*
[d] *Department of Chemical Systems Engineering, The University of Tokyo, 7-3-1 Hongo, Bunkyo-ku, Tokyo 113, Japan*

Received 15 April 2007; revised 7 June 2007; accepted 9 June 2007
Available online 20 July 2007

Through the use of titania–tin oxide nanocomposites, an enhanced anatase-to-rutile phase transformation is achieved, while avoiding appreciable particle growth. Upon the addition of SnO_2, the phase transformation temperature fell, reaching a minimum value at 18 vol.% of tin oxide, before increasing. Neither anatase nor rutile phase particles showed exaggerated growth. SnO_2 particles demonstrated both transformation-enhancing and growth-retarding roles.

Keywords: Titania; Nanostructured materials; Phase transformation; Anatase; Nanocomposites

Nanostructured titanium dioxide-based ceramics, as photocatalytic and photovoltaic solar cell material, have stimulated tremendous interest in recent years; in particular, their importance in the field of energy conversion has increased considerably in the past few years due to ever-surging energy prices [1–3]. One of the prerequisites for effectively using nanostructured titania for these applications is to understand the science behind tailor-making nanostructures with respect to crystal structure (phase), grain size and porosity (or density) [3–23]. Almost all synthetic techniques for preparing nanostructured titania yield the metastable anatase phase [3–23]. On further heat treatment, anatase will convert to the stable rutile phase [3–8,11–23]. This transformation is invariably associated with drastic grain growth and the eventual destruction of the "nanostructuredness" of the material [3–8,11–23]. Converting the anatase phase to the stable rutile phase without undergoing drastic grain growth and porosity reduction is a major challenge [3–8,11–23]. In this paper we show, for the first time, that, unlike other anatase-to-rutile phase transformation enhancement techniques [7], tin oxide present as second phase particles effectively enhances anatase-to-rutile phase transformation and at the same time retards particle growth and porosity reduction.

Titania-based nanocomposites with 3–36 vol.% of SnO_2 were prepared from respective sols. Titania (anatase) and SnO_2 (rutile-type) aqueous sols were obtained from Taki Chemical Company, Kakogawa City, Japan. Both the sols were stabilized using ammonia with a final pH of 10. The primary particle size in the titania and tin oxide sols were 10 and 3 nm, respectively. The nanocomposites were made by simply mixing required amounts of SnO_2 sol and titania sol using a magnetic stirrer. After mixing, the mixed sol was dried at 110 °C for 12 h. The dried gel pieces were about 1000 μm in thickness. These samples were calcined at different temperatures and then subjected to differential thermal analysis (DTA), X-ray diffraction (XRD) and field emission-scanning electron microscopy (SEM) studies. The relative amount of rutile present in the samples has been calculated using the following equation [5,22,24]:

$$W_R = 1/[1 + 0.8(I_A/I_R)], \quad (1)$$

* Corresponding author. Address: University of Texas at Dallas, Richardson, TX 75083, USA. Tel.: +1 214 387 8819; e-mail: padmakumar.nair@gmail.com

1359-6462/$ - see front matter © 2007 Acta Materialia Inc. Published by Elsevier Ltd. All rights reserved.
doi:10.1016/j.scriptamat.2007.06.039

where W_R, I_A and I_R are the fraction of rutile, integrated intensities of the (101) peak of anatase and the (110) peak of rutile, respectively. The crystallite size of both anatase and rutile crystallites were calculated using the Scherrer relation:

$$D_{hkl} = K\lambda/(B_{hkl}\cos\theta), \quad (2)$$

where D_{hkl} is the crystallite size and K is a constant (in the present case, a value of 1.38 was assumed) [22]. λ is the wavelength of the CuKα line and B_{hkl} is the full width at half maximum. 2θ is the peak angle. The integrated intensities and peak widths were calculated using a pattern fitting technique to correct for the instrument- and wave length related broadening.

DTA of pure titania used in this study gave a very broad peak, above 900 °C, corresponding to the anatase-to-rutile transformation, whereas the SnO_2-containing nanocomposites showed sharp peaks indicating enhanced transformation to rutile. Figure 1 gives the phase transformation temperature for the nanocomposites obtained from the DTA data for various volume fractions of SnO_2 in the composite. In order to improve accuracy, for every sample at least two DTA runs were performed. With an increasing amount of SnO_2, the anatase-to-rutile transformation temperature first decreased to 848 °C for titania containing 18 vol.% of tin oxide and then increased to 856 °C for 30 vol.% of SnO_2. Up to 18 vol.% of SnO_2, the relative amount of rutile in the samples increases with increasing vol.% of SnO_2 and then decreases as shown in Table 1. XRD patterns of pure titania and the nanocomposites after heating at 750 °C for 8 h are given in Figure 2. All the major anatase and rutile peaks are marked "A" and "R", respectively. At 750 °C pure titania remains as anatase. In the case of nanocomposite samples, the transformation has already started and the extent of the transformation depends on the amount of SnO_2 present in the composite.

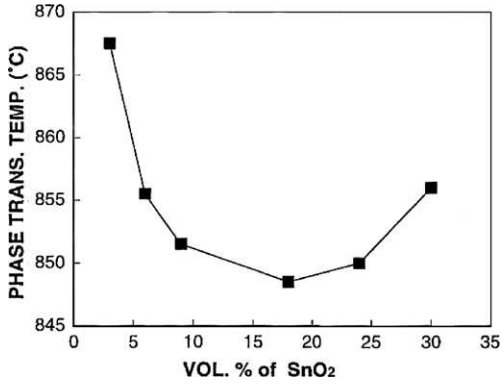

Figure 1. Vol.% of SnO_2 vs. anatase-to-rutile transformation temperature obtained from DTA for a heating rate of 20 °C min^{-1}.

Table 1. Relative amounts of anatase and rutile present in the samples and their crystallite sizes after heating at 750 °C for 8 h

Vol.% of SnO_2	% of rutile	Crystallite size of anatase (nm)	Crystallite size of rutile (nm)
0 (Pure titania)	0	56	(No rutile phase present)
3	67	39	64
6	84	35	62
18	95	28	53
24	94	27	49
36	74	26	37

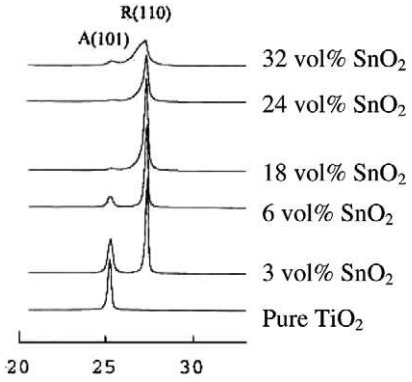

Figure 2. XRD patterns of pure and SnO_2 containing nanocomposites after heating at 750 °C for 8 h.

Table 1 gives the relative amounts of anatase and rutile present and their crystallite sizes in pure and SnO_2 containing nanocomposites heated at 750 °C for 8 h calculated using the above equations. With samples containing at least 18 vol.% of SnO_2, the (110) peak of pure SnO_2 ($2\theta = 26.4$) was also present in the XRD pattern and overlapped with the (110) peak of rutile. These overlapping peaks were separated using a pattern fitting technique for accurately determining the integrated intensities of (110) peak of rutile. Figure 3 presents the SEM micrographs of pure titania, pure SnO_2 and titania nanocomposites containing 3–18 vol.% SnO_2 after heating at 800 °C for 8 h. Pure titania has completely transformed rutile and does not show any porosity, but the titania phase of the nanocomposite is still porous. The larger crystallites are rutile titania and the smaller particles are SnO_2 second phase particles. Even though the SEM micrograph of the composites clearly showed a two-phase nanocomposite, there can be some degree of solid solution formation at the neck region (contact points) between the titania and the tin oxide particles. However, the TiO_2–SnO_2 system undergoes spinodal decomposition [25–27] and if the composition at the neck region is in the range of 10–90 mol.% of SnO_2, the system will remain as a two-phase mixture below 900 °C because of the spinodal reaction [25–27].

In the titania–tin oxide nanocomposite, tin oxide has a dual role. SnO_2 second phase particles accelerate the anatase-to-rutile transformation by providing a crystallographically similar surface which reduces the surface energy requirement for the formation of the critical nuclei of rutile phase. Crystal structure of tin oxide is tetragonal (rutile type) with very similar lattice parameters. For SnO_2 $a = 0.4737$ and $c = 0.3186$ nm and for rutile TiO_2 $a = 0.4593$ and $c = 0.2958$ nm. Lattice parameter mismatch in a and c are only around 3.04% and 7.15%, respectively. Therefore, SnO_2 may act as a semicoherent surface for the transforming rutile to grow

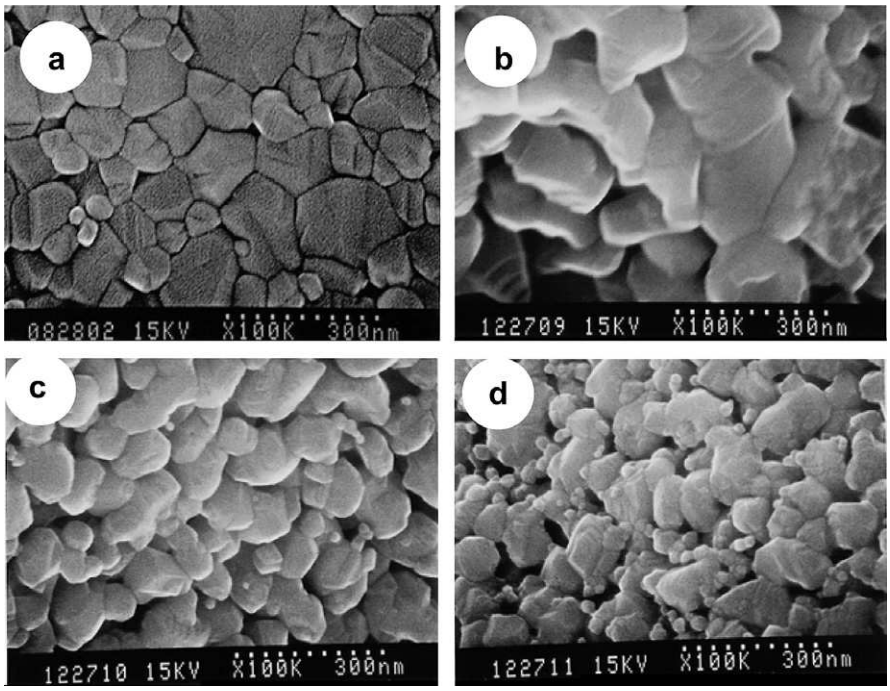

Figure 3. SEM micrographs of (a) pure titania, (b) titania–3 vol.% SnO_2, (c) titania–9 vol.% SnO_2, and (d) titania–18 vol.% SnO_2 nanocomposite after heating at 800 °C for 8 h.

"epitaxially" on it. However, there is no direct evidence to support this claim.

This can be inferred from the following equations describing the relationship between critical nuclei size and interfacial energy of new phase [23,28]:

$$\Delta G = \tfrac{4}{3}\pi r^3 \Delta G_{\mathrm{CHEM}} + \tfrac{4}{3}\pi r^3 \Delta G_{\mathrm{STRAIN}} + 4\alpha\pi r^2 \gamma_{\mathrm{AR}} + 4\beta\pi r^2 \gamma_{\mathrm{RT}} + 4\delta\pi r^2 \gamma_{\mathrm{RG}}, \quad (3)$$

where ΔG, ΔG_{CHEM}, $\Delta G_{\mathrm{STRAIN}}$, γ_{AR}, γ_{RT} and γ_{RG} are the change in total free energy, Gibbs free energy, strain energy, anatase–rutile interfacial energy, rutile–tin oxide interfacial energy and rutile–air interfacial energy, respectively. α, β and δ are the fraction of interfacial area covered by anatase–rutile, rutile–tin oxide and rutile–air, respectively ($\alpha + \beta + \delta = 1$). The critical nuclei size, r_c, is given by:

$$r_c = -2\left[\frac{\alpha\gamma_{\mathrm{AR}} + \beta\gamma_{\mathrm{RT}} + \delta\gamma_{\mathrm{RG}}}{\Delta G_{\mathrm{CHEM}} + \Delta G_{\mathrm{STRAIN}}}\right]. \quad (4)$$

The higher volume fraction of SnO_2 particles in the composite may be providing a larger number of easy nucleation sites. Also the rutile–tin oxide interfacial energy, γ_{RT}, will be much smaller than the other two interfacial energies due to the crystallographic similarity between rutile and tin oxide. A higher volume fraction of tin oxide will also increase β ($\beta = 1 - \alpha - \delta$), resulting in smaller contributions from γ_{AR} and γ_{RG}. This overall decrease in the numerator will result in a smaller critical nuclei size, r_c. If this were the only mechanism operating, the DTA phase transformation temperature should decrease continuously and reach a minimum plateau with an increased amount of SnO_2 second phase particles. In reality, this did not happen (see Fig. 1). Up to 18 vol.% of SnO_2 second phase, the DTA transformation temperature indeed decreased and after that it started to increase, indicating a retardation in phase transformation.

This effect can be understood by considering the role of SnO_2 as a "second phase stabiliser". The second phase stabilization effect is purely physical in nature. The most probable mechanism among the four different mechanisms stated under the physical stabilization effect [5,21] is the lowering of coordination in the matrix phase by the SnO_2 second phase [29,30]. With more and more SnO_2 particles in the composite, the number of titania particles having actual physical contact with neighbouring titania particles will decrease. This decrease in titania–titania contacts per unit volume will retard grain growth [21,29,30] and eventually the matrix phase's ability to reach critical nuclei size for the transformation to take place [4,11,23]. This can be seen from the crystallite size data given in Table 1 and the DTA phase transformation data shown in Figure 1. This slowing down of grain growth will retard the phase transformation processes by reducing the chance for achieving the critical nuclei size. This can be explained as follows: in a nucleation growth type of transformation like this one, the very first step is embryo formation. The embryo becomes stable only after reaching the critical size, called the critical nuclei size, as given by Eq. (4). From the sintering and grain growth points of view, the rate at which the embryo can grow to the critical nuclei size depends on the number of nearest titania neighbours (subcoordination number). With the increase in the volume fraction of SnO_2 particles in the nanocomposite, the following will happen:

1. The number of titania particles having actual physical contact with a SnO_2 particle will increase.

2. The titania–titania coordination in the matrix phase (sub-coordination) will decrease.

The first effect will enhance the anatase-to-rutile transformation by providing a suitable surface for the rutile phase to grow on. The second effect will retard the transformation by preventing aggregation and grain growth of titania particles. As can be seen from Table 1, with an increase in the amount of SnO_2, growth of both anatase and rutile crystallites are retarded. A slow grain growth will increase the time taken for the embryo to reach the critical nuclei size. These two effects are opposing, the second effect taking over the first at about 18 vol.% of SnO_2, as can be seen from Figures 1 and 2 and Table 1. It is interesting to note that effective retardation of both anatase and rutile crystallite growth is observed in all the composites even though up to 18 vol.% of SnO_2 there is clear enhancement in the anatase-to-rutile transformation.

From the above results it is clear that nanocomposite formation with a carefully selected second phase is an effective technique to enhance metastable-to-stable phase transformation and at the same time retard particle growth. The selection criteria for the second phase are:

a. It should enhance phase transformation by providing active nucleation sites thereby reducing the interfacial energy necessary for nucleation.
b. It should be relatively inert to physically stabilize the matrix phase by spatially separating the primary particles in the matrix phase so that it will limit the ability of primary particles in the matrix phases.

This technique could be applied to stabilizing other nanostructured systems too.

Authors are thankful to Jeff Hicks of the University of Twente, The Netherlands for useful discussions.

[1] M.S. Dresselhaus, I.L. Thomas, Nature 414 (2001) 332.
[2] M. Grätzel, Nature 414 (2001) 338.
[3] K-N.P. Kumar, K. Keizer, A.J. Burggraaf, T. Okubo, H. Nagamoto, S. Morooka, Nature 358 (1992) 48.
[4] D.J. Reidy, J.D. Holmes, M.A. Morris, J. Eur. Ceram. Soc. 26 (2006) 1527.
[5] K-N.P. Kumar, Appl. Catal. 119 (1994) 163.
[6] Y. Iida, S. Ozaki, J. Am. Ceram. Soc. 44 (1961) 120.
[7] J. Nair, P. Nair, F. Mizukami, Y. Oosawa, T. Okubo, Mater. Res. Bull. 34 (1999) 1275.
[8] K-N.P. Kumar, K. Keizer, A.J. Burggraaf, J. Mater. Chem. 3 (1993) 917.
[9] R. Lee Penn, J.F. Banfield, Am. Mineral. 84 (1999) 871.
[10] H. Zhang, J.F. Banfield, J. Mater. Res. 15 (2000) 437.
[11] D.J. Reidy, J.D. Holmes, M.A. Morris, Ceram. Int. 32 (2006) 235.
[12] K. Kranthi, K.K. Akurati, S.S. Bhattacharya, M. Winterer, H. Hahn, J. Phys. D: Appl. Phys. 39 (2006) 2248.
[13] J.H. Lee, Y.S. Yang, J. Mater. Sci. 40 (2005) 2843.
[14] Z.M. Shi, W.G. Yu, X. Bayar, Scripta Mater. 50 (2004) 885.
[15] M. Zaharescu, M. Crisan, L. Simonescu, D. Crisan, M. Gartner, J. Sol-Gel Sci. Technol. 8 (1997) 249.
[16] P. Nair, J. Nair, E.B.M. Doesburg, J.G. van Ommen, J.R.H. Ross, A.J. Burggraaf, Y. Oosawa, F. Mizukami, J. Porous Mater. 6 (1999) 69.
[17] K-N.P. Kumar, J. Kumar, K. Keizer, J Am. Ceram. Soc. 77 (1994) 1396.
[18] K-N.P. Kumar, K. Keizer, A.J. Burggraaf, T. Okubo, H. Nagamoto, J. Mat. Chem. 3 (1993) 923.
[19] P. Nair, F. Mizukami, J. Nair, M. Salou, Y. Oozawa, H. Izutsu, K. Maeda, T. Okubo, Mater. Res. Bull. 33 (1998) 1495.
[20] K-N.P. Kumar, K. Keizer, A.J. Burggraaf, J. Mater. Sci. Lett. 13 (1994) 59.
[21] P. Nair, F. Mizukami, T. Okubo, J. Nair, K. Keizer, A.J. Burgraaf, AIChE J. 43 (11A) (1997) 2710.
[22] K-N.P. Kumar, K. Keizer, A.J. Burggraaf, J. Mat. Chem. 3 (1993) 1141.
[23] K-N.P. Kumar, Scripta Metall. Mater. 32 (1995) 873.
[24] R.A. Spurr, H. Myers, Anal. Chem. 29 (1957) 760.
[25] W.D. Kingery, H.K. Bowen, D.R. Uhlmann, Introduction to Ceramics, second ed., Wiley, New York, 1976, p. 425.
[26] T.C. Yuan, A.V. Virkar, J. Am. Ceram. Soc. 69 (1986) C-310.
[27] J-H. Lee, S-J. Park, J. Mater. Sci. (Mater. Elec.) 4 (1993) 254.
[28] H.K.D.H. Bhadeshia, A.L. Greer, in: Z. Barber (Ed.), Introduction to Materials Modelling, Maney Publishing, London, 2005, p. 76.
[29] E.G. Liniger, R. Raj, J. Am. Ceram. Soc. 71 (1988) C-408.
[30] K-N.P. Kumar, J. Kumar, K. Keizer, T. Okubo, M. Sadakata, J.J. Engell, Mater. Sci. Lett. 14 (1995) 1784.